Tunneling Spectroscopy of Overdoped $Bi_2Sr_2CaCu_2O_{8+\delta}$ Single Crystals

Lutfi Ozyuzer[1,2,3], John F. Zasadzinski[1,2], Chris Kendziora[4] and Kenneth E. Gray[1]
[1] *Science and Technology Center for Superconductivity and Materials Science Division, Argonne National Laboratory, Argonne IL 60439*
[2] *Illinois Institute of Technology, Chicago, IL 60616*
[3] *Department of Physics, Izmir Institute of Technology, TR-35230 Izmir, Turkey*
[4] *Naval Research Laboratory, Washington DC 20375*

The point contact tunneling technique is used to examine quasiparticle and Josephson currents in overdoped $Bi_2Sr_2CaCu_2O_{8+\delta}$ (Bi-2212) single crystals with bulk T_c values near 62 K. High quality superconductor-insulator-normal metal (SIN) tunnel junctions are formed between Bi-2212 crystals and a Au tip, which display well-resolved quasiparticle gap features including sharp conductance peaks. Reproducible superconductor- insulator-superconductor (SIS) tunnel junctions are also obtained between two pieces of the Bi-2212 crystals, resulting in simultaneous quasiparticle and Josephson currents. Superconducting gap values are obtained from the SIS data using a model with d-wave symmetry. The SIS tunneling conductances also show very pronounced symmetric dips and humps at high bias voltages. The high bias conductance data reveal that the dip and hump features are part of a larger spectrum that extends out to 300-400 mV. The dynamic conductances of both SIN and SIS junctions are qualitatively similar to those found on optimally-doped Bi-2212 but with reduced gap values (Δ=15-20 meV). The maximum Josephson current depends on junction resistance in a manner consistent with Ambegaokar-Baratoff theory but with a reduced I_cR_n product of $\sim$2.4 mV.

PACS numbers: 74.50.+r, 74.80.Fp, 74.72.Hs, 74.62.Dh

I. INTRODUCTION

Many of the early studies on the high-T_c superconductors (HTS) focused on the physical and chemical properties of optimally-doped compounds where the critical temperature, T_c, is the highest value. Recently, the doping dependence of the HTS has become a significant issue due to its peculiar influence on superconducting properties such the energy gap1 and spectral features of the tunneling density of states (DOS). [1,2] One question that arises is how the pairing symmetry is affected by doping. The symmetry of the superconducting order parameter for the optimally-doped HTS is consistent with $d_{x^2-y^2}$ (d-wave) as found in angle resolved photo emission spectroscopy (ARPES) [3,4] experiments on $Bi_2Sr_2CaCu_2O_{8+\delta}$ (Bi-2212) and tricrystal ring [5,6] experiments on $YBa_2Cu_3O_{7-x}$ and $Tl_2Ba_2CuO_{6+\delta}$. The possibility of gap symmetry conversion from d-wave to s-wave with overdoping of Bi-2212 is suggested by Kendziora et al. [7] and Kelley et al. [8] using Raman and ARPES studies respectively. Tunneling measurements of the strong coupling ratio, $2\Delta/k_BT_c$, in Bi-2212 indicate a decrease from a value of 9.3 for optimally doped samples to values approaching the BCS mean field value with overdoping. [1] It thus has become clear that the overdoped region of HTS is interesting in its own right and in this article we focus on tunneling spectroscopy measurements on overdoped crystals of Bi-2212. The principal result is that the tunneling spectra are qualitatively similar to those found on optimally-doped crystals, but with a reduced energy scale, i.e. typical Δ values are 15 meV-20 meV compared to 38 meV for optimal doping. [1,2]

The optimally-doped compound of Bi-2212 has a T_c onset of 95 K and its T_c can be reduced either by additional oxygen content (overdoping) or by the removal of oxygen with vacuum annealing (underdoping). [1,2,9] Thus, Bi-2212 is a perfect candidate for studying its physical properties over a large range of the doping phase diagram. Furthermore Bi-2212 can be grown as a single crystal with a very low defect density and a very flat surface after cleaving making it suitable for surface sensitive experiments such as scanning tunneling microscopy (STM), Raman, and ARPES.

Tunneling spectroscopy is one of the most powerful methods for studying the DOS near the Fermi level. [10] Measurements on planar junctions have revealed detailed information about electron-phonon interactions in conventional superconductors. [11] The reliability of point contact tunneling (PCT) spectroscopy has been proven for conventional superconductors [12] such as Nb where the strong coupling phonon structures have been observed similar to that found in planar junctions. PCT and STM generally measure a spatially local density of states near the Fermi level on both conventional and HTS. [10] Due to the larger contact area of the PCT method, local variations in oxygen stoichiometry are expected to have a smaller effect than with an STM. In general, tunneling studies of Bi-2212 by PCT [1,2] and

STM [2,13,14] have shown that the spectra are very similar. The short coherence length and anisotropic structure of the HTS present significant obstacles to obtaining clear tunneling effects. Tunneling requires a pinhole-free, insulating, homogeneous barrier and clean electrode surfaces. The larger junction area of planar junctions increases the probability of finding pinholes and/or other defects and the resulting junction produces complex and unexplainable spectra in many cases. [15] More than a decade has passed since the discovery of HTS and there are still no reproducible planar junctions which show the same high quality characteristics as observed in PCT or STM.

Near-optimal doped Bi-2212 has been examined by a variety of tunneling methods [10] including break junctions [1,16,17] , PCT [1,2,18] and STM [1,2,13,14,19] and there is a wide scatter in the measured values of the superconducting gap parameter, Δ. Reported values of Δ range from 20 meV to 50 meV. [10] Recent measurements by STM, PCT and break junctions [1,2] on high quality crystals show that this wide spread is likely due to the sensitive dependence of the superconducting gap on hole doping which tends to exacerbate problems associated with inhomogeneous doping or surface effects. Because of better understanding of HTS chemistry and fabrication, the quality of Bi-2212 crystals has improved considerably. Better control of purity of the crystal narrows the spectrum of obtained energy gap values for a given doping level and now it can be safely stated that for optimally-doped Bi-2212 with a T_c onset of 95 K, Δ is close to 38 meV. [2] This improved reproducibility has allowed the observation by PCT and break junctions of a remarkable effect whereby the superconducting gap in Bi-2212 changes substantially and monotonically with doping over a narrow doping region where the T_c has a maximum. [1] On the overdoped side this effect has been seen by STM as well. [2,13,14,19]

In this paper, we report point contact tunneling measurements on single crystals of heavily-overdoped Bi-2212 single crystals with bulk T_c near 62 K. Some of the results have been published in Ref. 1 cited above, but here we present a more detailed examination of the spectra. The tunneling spectra from both superconductor-insulator-normal metal (SIN) and superconductor-insulator-superconductor (SIS) junctions exhibit the same qualitative features as found on optimally-doped crystals but with a reduced gap size. Typical spectral features of SIN junctions include a weakly decreasing background conductance, asymmetric conductance peaks, and a dip/hump structure at high bias. The SIS junctions exhibit a well-defined Josephson current when the junction conductance exceeds a critical value of about 10 μS and measurements of the Josephson I_c vs.R_n are presented over two decades of junction resistance, R_n. For two SIS junctions which exhibit clean quasiparticle conductances a comparison is made between two model fits to the data: a smeared BCS DOS and a momentum-averaged d-wave DOS. We find that the d-wave fit is in better agreement with the sub-gap region but that neither model adequately fits the data beyond 2Δ.

II. EXPERIMENT

Samples of single crystal Bi-2212 were grown by a self-flux technique in a strong thermal gradient to stabilize the direction of solidification. Overdoping has been accomplished using stainless steel cells sealed with samples immersed in liquid oxygen, as described elsewhere. [9] Tunneling measurements were performed on crystals with T_c nearly 62 K, and a transition width of about 1 K. Magnetization measurements were taken after each tunneling measurement, and no significant change of T_c has been observed. Tunneling measurements were done with the apparatus [20] cooled by ^{4}He exchange gas coupled to a liquid helium bath. Cleaved single crystal samples of overdoped Bi-2212 usually have shiny surface on the a-b plane. Each is mounted on a substrate using an epoxy so that the tip approaches along the c-axis. Normally a Au tip was used as a counter-electrode, and it was mechanically and chemically cleaned before each run.

The SIN and SIS junctions are formed as follows. After the sample is placed in the measurement system and cooled down to 4.2 K, the distance and contact force between the tip and sample are adjusted using a differential micrometer. In the ordinary way, a tip pushes onto the surface of the crystal and a stable mechanical junction forms between the tip and crystal. Here the insulating tunnel barrier is the native surface layer of the crystal. The two neighboring Bi-O planes in Bi-2212 have weak bonds compared to Cu-O and Sr-O layers. Therefore the cleaved surface of Bi-2212 is a single Bi-O plane and presumably the barrier is due to this layer and the underlying Sr-O layer. STM studies have indicated that this surface layer is semiconducting with an energy gap of at least 100 meV. [15] While the tip is pushed against the crystal, the I-V curve is continuously monitored on an oscilloscope until a suitable junction is obtained. Such junctions clearly display a superconducting gap in the I-V characteristics. The junction resistances range from 300 Ω to 50 kΩ for the SIN junctions but the majority of junctions fall in a narrower range $\sim$ 2k Ω-10 kΩ. Although the tip approaches nominally along the c-axis the tunneling direction is not known with certainty, but we will argue later that both the SIN and SIS junctions have the tunnel barrier perpendicular to the c-axis. The junction area is also not known with certainty, however, a good estimate is found from similar PCT measurements of Nb [12] where the barrier height analysis of the tunneling conductance led to a contact diameter of $\sim$2400 $\mathring{A}$.

Increasing the force of the tip against the crystal produces an ohmic contact (∼1 Ω) between the tip and crystal, likely due to a perforation of the barrier layer. This results in a mechanical bond between Au and Bi-2212 because when the tip is elevated, often a piece of Bi-2212 crystal also goes up that is fastened to the tip. We have found that it is not necessary to raise the tip to form an SIS junction but merely to relieve the pressure. Presumably in this case one of the Bi-O plane pairs are separated and this results in an SIS junction, which forms between different parts of the crystal. The dislodged piece probably remains in the cavity in the larger crystal as these SIS junctions are mechanically very stable. As a consequence this technique provides a fresh junction that is formed in-situ deep in the crystal, thereby minimizing the exposure of the surface. A schematic of the SIS junction between two pieces of crystal is represented in Fig. 1. The junction area is uncertain, however, for a rough idea, the size of the attached crystallite is on the order of 10-100 μm on edge so this provides an upper bound to the area. SIS junction resistances are again in the range, 2 kΩ to 120 kΩ so this indicates that the actual contact area is considerably less than 10 μm on edge. The first derivative measurements, σ=dI/dV, were obtained using a Kelvin bridge circuit with the usual lock-in procedure. I(V) and dI/dV(V) were simultaneously plotted on a chart and recorded on computer.

The SIN junctions and SIS junctions were easily identified by their characteristic tunneling conductances. SIN junctions display an asymmetric, weakly decreasing background, an asymmetric dip/hump feature and as low as 10% - 15% zero bias conductance. The SIS junctions have a symmetric background, less than 1% zero bias conductance, symmetric dip and hump features and conductance peaks at 2Δ. In addition the SIS junctions exhibit a hysteretic Josephson current when the junction resistance is below 100 kΩ.

III. RESULTS OF SIN JUNCTIONS

Before showing the experimental results, we review here the basic theoretical approach to analyzing the tunneling data. The tunneling current in an SIN junction can written as, [11]

$$I(V) = c \int |T|^2 N_{sn}(E) N_{nn}(E+eV)[f(E) - f(E+eV)]dE \tag{1}$$

where $f(E) = [1 + exp(E/k_BT)]^{-1}$ is the Fermi function, $N_{sn}(E)$ is the DOS of the superconductor, $N_{nn}(E)$ is DOS of the normal metal which is Au in our case, $|T|^2$ is the tunneling matrix element, and c is a proportionality constant. The quasiparticle energy is given by E, which is defined relative to the Fermi level. For a rough estimation of the tunneling current, we may assume that N_{nn} is a constant near Fermi level and tunneling matrix element, $|T|^2$, has weak energy dependence over the voltage range of the energy gap. Then,

$$dI/dV \equiv \sigma_s = c|T|^2 N_{sn}(E) = c|T|^2 N_s(E) N_n(E) \tag{2}$$

where we have now set $E = eV$. $N_s(E)$ is the superconducting part of the DOS, and $N_n(E)$ is normal state DOS of superconductor. In most low-T_c superconductors, $N_n(E)$ usually is a constant over the energy range of interest. The ratio of σ_s/σ_n gives the superconducting DOS. According to BCS theory, the superconducting DOS is

$$N_s(E) = \begin{cases} Re[\frac{E}{\sqrt{E^2-\Delta^2}}] & |E| \geq \Delta \\ 0 & |E| < \Delta \end{cases} \tag{3}$$

For conventional superconductors, the energy gap, Δ, is a constant in $\mathbf{k}$ space (isotropic s-wave pairing symmetry). However, for superconductors with d-wave pairing symmetry, the energy gap is anisotropic on the Fermi surface. In a two dimensional superconductor, a simple d-wave DOS suggested by Won and Maki [21] is given by

$$N_s(E, \mathbf{k}) = \mathrm{Re}\left\{ \frac{E - i\Gamma}{\sqrt{(E - i\Gamma)^2 - \Delta(\mathbf{k})^2}} \right\} \tag{4}$$

where $\Delta(\mathbf{k}) = \Delta_0 \cos(2\phi)$ is the k dependent energy gap and ϕ is the polar angle in k-space. The DOS, $N_s(E)$, is found by an integral over the polar angle ϕ. Here, E is replaced by $E - i\Gamma$, where Γ is a smearing parameter to account for quasiparticle lifetime. [22]

Figure 2 shows the dynamic conductances of three SIN junctions at 4.2 K (dots) obtained from three different crystals. Negative voltage corresponds to removal of electrons from the superconductor, or occupied quasiparticle states in the DOS. Each junction displays sharp conductance peaks near 20 mV and a decreasing background conductance out to 200 mV. Figure 2(a) and 2(b) display a very pronounced dip and hump for negative bias that is also seen

in tunneling studies [1,2,13,14] of optimally-doped Bi-2212 and is consistent with ARPES [3,4] measurements of the spectral weight function along the (π,0) momentum direction. This dip feature is located at approximately twice the voltage of the conductance peak and hence is scaling with the superconducting gap itself. A possible explanation for the origin of the dip feature is given in Ref. 2. The zero bias conductances vary from 20% to 40% of the estimated normal state conductance but in a few cases we have seen values as low as 10%-15% in overdoped crystals.

The tunneling conductance in Fig. 2(c) is deliberately chosen to demonstrate the general features of a junction with a relatively low resistance, about 300 Ω in this case. Such a low resistance means that we are approaching the point contact situation where Andreev reflection [23] may be taking place and this might explain the more sharply increasing conductance as zero bias is approached. Kashiwaya et al. [24] calculated the differential conductance of a normal metal-insulator-(d-wave) superconductor junction within the framework of the BTK theory [25] which includes tunneling and Andreev reflection. Further study is needed to fit Fig. 2(c) and other low resistance junctions to the theory, which is beyond the scope of this paper. However we note that a general feature of this model [24] is the presence of a sharp zero-bias conductance peak in the superconducting state when the tunnel barrier is perpendicular to the Cu-O planes of HTS. Since we never observe this feature, this seems to suggest that our SIN junctions all have the barrier parallel to the Cu-O planes, as would result if it originates from the native Bi-O layer on the cleaved crystal surface.

Because of large upper critical fields [26] of HTS, the normal state conductance cannot be obtained experimentally. Somehow we have to estimate normal state conductance. Since we expect the superconducting and normal state conductances to merge at voltages much higher than the gap, we can extrapolate the values of σ_s at high voltages and get an approximation, σ_n*, thus obtaining an approximate DOS from the ratio of σ_s/σ_n*. We used a simple polynomial fit to obtain σ_n* and checked the resulting normalized conductance to make sure that the sum rule of the DOS was verified. The solid lines in the Fig. 2 represent estimated normal state conductance curve using this procedure.

When the superconducting dynamic conductance is divided by σ_n*, we obtain the normalized conductances [dots in Fig. 3], which can be compared to theory to find the energy gap of the superconductor. Note that the dip features still exist after normalization and in the case of Fig. 3(c), the dips are now evident whereas they were obscured in the raw conductance data. In Fig. 3, solid lines correspond to fits from eq. (1) using a smeared BCS DOS i.e. Eq. (3) with the inclusion of a quasiparticle lifetime term, Γ. Energy gaps vary from 15 to 20 mV for the SIN junctions. Figure 3(a) shows a good overall agreement with the smeared BCS DOS while Fig. 3(b) and Fig. 3(c) show a sub-gap conductance that is more cusp-like and suggestive of d-wave symmetry. Fits of the data in Fig. 3(b) to a d-wave DOS as in eq. (4) lead to an identical value for Δ (19 meV) which is then interpreted as the maximum of $\Delta(\mathbf{k})$. This range of sub-gap shape from d-wave-like to smeared s-wave-like was also observed [2] in optimally-doped Bi-2212 and one possible explanation has to do with tunneling directionality effects. [27] For optimally-doped samples, reproducible energy gaps are found [1,2] near 38 meV corresponding to $2\Delta/k_BT_c \sim 9.3$. This is very large when compared to a BCS ratio of 4.28 for a d-wave superconductor. [21] In the overdoped samples, we obtained $2\Delta/\mathrm{k}_B\mathrm{T}_c$ in the range of 5.6-7.5. The energy gap decreases rapidly when T_c goes from 95 to 62 K and the trend is to approach the BCS mean-field gap value. This rapid decrease of the gap with increased hole doping is also seen in ARPES experiments [28] and STM measurements [2,14] on overdoped Bi-2212.

IV. RESULTS OF SIS JUNCTIONS

If both electrodes are identical superconductors in eq. (1) the quasiparticle conductance peaks are at $\pm 2\Delta$. As a result of the convolution of the superconducting DOS, the quasiparticle peaks are sharper and zero bias conductances are lower than SIN junctions. The Fermi function effect is very small compared to SIN junctions. In addition, Cooper pairs may tunnel through the barrier and a Josephson current occurs at zero bias in the I-V characteristics.

In this part of the paper, highly reproducible and stable SIS junctions will be examined. Figure 4(a), (b) and (c) show current-voltage characteristics of three junctions from three different crystals. These were measured at 4.2 K and the junctions indicate SIS type, with very low leakage currents and sharp current onsets at eV$\sim$40 meV which is twice the gap value found in the SIN junctions. They also exhibit a hysteretic Josephson current at zero bias. Figure 4(d) shows the sub-gap region of Fig. 4(c) on a more sensitive scale to clearly show the hysteretic nature of the Josephson current.

Figure 5 shows conductance-voltage characteristics of SIS junctions from three different samples at 4.2 K. The junction resistances are in the range 5 kΩ - 15 kΩ. Here the Josephson current gives rise to a very large conductance peak at zero bias which is off the scale. Peaks correspond to $\pm 2\Delta$ values. Symmetric dips are found near 3Δ as found on Bi-2212 crystals near optimal doping. [1,29] On average, the dip strength is low with respect to optimally-doped

samples. [1,2] The conductance at higher bias voltages ($e|V| > 3\Delta$) at first decreases with increasing bias, as found in the SIN junctions. This behavior exists out to $|V| \sim 300$ mV but for bias voltages beyond this value there is an upturn in the conductance. A similar upturn is also observed in break junctions of Bi-2212 by Mandrus et al. [16] In the simple approximation expressed in eq.(2), it is assumed that the tunneling matrix element, $|T|^2$, is energy independent. However, at very high bias voltages we are likely approaching the barrier height potential. As a consequence of this, the tunneling transmission probability is increasing and the barrier height effect which gives a parabolic increase in conductance [11] may become dominant beyond ±300 mV.

The fact that the upturn in conductance occurs at nearly the same bias value in these junctions as well as other break junctions [16] which can differ in resistance by two orders of magnitude strongly argues against extrinsic effects such as heating as the cause of the initial decreasing background between 100 mV and 300 mV. Rather, the data suggest that the dip and hump feature are part of a larger spectrum that includes a tail extending out to 300-400 mV and that all of these features are intrinsic effects of the quasiparticle DOS in Bi-2212. It should be noted that a similar dip-hump-tail feature is found in the quasiparticle spectral weight function, A($\mathbf{k}$,ω) measured in ARPES. [30] Although no definitive explanation of these spectral features exists, it is important to note the consistency between tunneling and ARPES.

In our preliminary analysis of these SIS data, the goal was to obtain the energy gap of the Bi-2212, and we used the simplest approach, which was to use Eq. (1) with a smeared BCS DOS for both electrodes. Furthermore, one of the key differences between s-wave and d-wave models of the SIS conductance is in the shape of the sub-gap region which is difficult to obtain experimentally because of the switching property of the Josephson current. Thus a detailed comparison of the two models for every junction is not fruitful and we found that an accurate estimate of 2Δ could be obtained directly from the conductance peak voltage. To demonstrate this, the data of Figs. 5(a) and 5(b) were normalized by a constant value which is the conductance at 150 mV. The normalized conductances are displayed in dots in Fig. 6(a) and 6(b). The steeper background shape in Fig. 5(c) did not allow us to normalize it with constant value, so we chose another junction (which was not measured to a high bias voltage) for normalization in Fig. 6(c). The solid lines in Fig. 6, represents SIS fits with the smeared BCS DOS and T=4.2 K. The Δ and Γ values are shown for each curve. Note that in each case the conductance peak voltage is exactly $2\Delta/e$. The quality of the fits in the sub-gap region varies but the significance of this is difficult to asses since switching of the Josephson current can introduce structural artifacts near zero bias. The principal result here is that the energy gap values (Δ= 16 meV - 18 meV) are consistent with those found in SIN junctions. Considering all of the SIS junctions (> 20) on the four different crystals, the full range of gap values was Δ = 15 meV - 20 meV.

Up to now, we used a simple smeared BCS DOS for analysis of the SIN and SIS conductance curves to obtain the energy gap of the overdoped Bi-2212. SIN and SIS fits gave consistent results and the energy gap was found to be dramatically smaller than that of optimally-doped Bi-2212. However, it is clear from the fits in Figures 3 and 6 that a smeared BCS DOS does not adequately fit the data in each case. Given the expected d-wave symmetry of the gap in Bi-2212, we analyzed some of the conductance data using the simple d-wave model of Eq. 4. We focus on SIS junctions because it is in these types of junctions that the differences between d-wave and smeared s-wave are most clearly observed. Furthermore, we choose relatively high resistance junctions where the effects of the Josephson current are minimized.

The inset of Fig.7 shows another SIS tunneling conductance which is particularly clean. The Josephson current was very low for this particular junction due to its higher resistance (∼40 kΩ) and a relatively small zero bias conductance peak is observed. To obtain the sub-gap conductance very clearly, the d.c. bias current was swept very slowly inside the gap in both directions. These data also display generic Bi-2212 quasiparticle tunneling conductance characteristics such as sharp quasiparticle peaks, and a dip/hump feature at high bias. Because the data are symmetric with bias polarity, we focus only on the positive bias side of the spectrum. Our goal is to examine to what extent the shape of the sub-gap conductance reveals information on pairing symmetry. Thus we consider the simple d-wave model of eq. (4) for comparison to the smeared BCS model.

The solid line in Fig. 7 corresponds to the estimated normal state conductance, σ_n*. It is obtained after masking the data below 100 mV and fitting with a 3rd order polynomial curve. The dots in Fig. 8 show the normalized tunneling conductance curve from Fig. 7 and the solid line is the smeared BCS fit, including Γ, which is obtained from Eq. (1) with T=4.2 K to obtain the SIS tunneling conductance. The value of 2Δ=35 meV is consistent with the other junctions and as noted above could have been obtained directly from the conductance peak voltage. The overall quality of the fit is poor. The smaller peak in the BCS fit near Δ arises from the Γ parameter and while the data do not show such a distinct feature there is clearly a broadened peak in this region. The dip/hump feature is not reproduced in this simple model.

Before discussing the d-wave fit of the data, it is useful to present the generic features of the simplest model. Figure 9(a) shows a generated DOS curve for d-wave symmetry using Eq. (4). The underlying assumptions are that the

Fermi surface is isotropic and the probability of tunneling is same for all k directions. The cusp feature at zero bias is the basic indication of d-wave pairing symmetry. The SIS tunneling conductance curve is obtained with convolution of Fig. 9(a) with itself using Eq. (1), with T=4.2 K, and this is shown in Fig. 9(b). Note that the peak height to background (PHB) ratio is ~ 2 for the model d-wave SIS tunneling conductance whereas the normalized SIS curves of Figs. 6 and 8 suggest a PHB ratio that is much higher than 2. Thus we see at the outset that this simple d-wave model will not fit our data. One possible consideration is that our estimated normal state curve is incorrect. While this cannot be ruled out, it is difficult to conceive of a normal state conductance that would bring the PHB ratio from a value of 4 or 5 down to a value of 2 as the d-wave model requires.

Another possibility is that one or more of the underlying assumptions of the simple model are incorrect. ARPES results reveal that Bi-2212 has arch like Fermi surfaces in the four corners of the Brillouin zone [30] and this suggests the possibility that particular regions of momentum space are more heavily weighted than others in the contribution to the tunneling current, either due directly to the band structure or to the tunneling matrix element. For this reason we include a weighting function, $f(\phi)$, to Eq. (4) as is in Refs. 31 and 32,

$$N_s(E,\phi) = f(\phi)\,\mathrm{Re}\left\{\frac{E-i\Gamma}{\sqrt{(E-i\Gamma)^2-\Delta(\phi)^2}}\right\} \tag{5}$$

Δ where $f(\phi) = 1 + \alpha cos(4\phi)$. and the angle ϕ is measured with respect to the (π,0) direction in the Brillouin zone. Here α is a directionality strength and the full quasiparticle DOS is obtained by integrating over ϕ. It should be emphasized that eq.(5) is a phenomenological expression and there is no rigorous derivation of this result, but it can be seen immediately that this weighting function will qualitatively reproduce some of the conductance features observed in the experiment. For example, the observation in some SIN junctions of a smeared BCS DOS shape to the gap region conductance may be attributed to a non-zero a value which more heavily weights contributions along the (π,0) direction where $\Delta(\mathbf{k})$ is largest and minimizes the contribution from the nodal directions. This weighting would also explain the large PHB ratios in SIS junctions since a smeared BCS DOS can exhibit a large PHB as shown in Fig. 8.

We fit the normalized SIS tunneling conductance, given in Fig. 8, using Eq. (5) and the solid line in Fig. 10 shows the resulting curve with Δ=17.5 meV, Γ=0.05, α=0.8. Note here that Δ is the maximum of $\Delta(\mathbf{k})$ and is the same magnitude as obtained with the BCS fit. For eV<2Δ, the experimental results and fit are in better agreement than for the BCS fit in Fig. 8. For eV > 2Δ the fit shows an abrupt drop from the peak to background that is not found in the data. This feature appears to be generic to d-wave models (see Fig. 9(b)) but we have never observed it in over 50 SIS junctions on Bi-2212 with various hole doping [1,2] and to our knowledge such an abrupt drop has never been seen in the literature. Rather the experimental data invariably exhibit a much broader conductance peak followed by the dip/hump feature which is not found in this simple d-wave model. The inset of Fig. 11 shows another SIS junction which was chosen for analysis because of the relatively low Josephson current and clean quasiparticle data. This junction exhibits a smaller PHB ratio than in Fig. 10. The solid line in the Fig. 11 is the estimated normal state conductance. The normalized data is displayed in Fig. 12 along with the fit obtained with the following parameters: Δ=19.5 meV, Γ=1.5, α=0.6. The larger Γ value reflects the generally broader features of this junction's spectrum and there is better agreement with data in the sub-gap region. Nevertheless, for eV>2Δ the data display the same deviation from the fit as found in Fig. 10. This suggests the possibility that these characteristics of the SIS spectra for eV>2Δ are intrinsic and not due to a less interesting effect such as a distribution of gap values due to sample inhomogeneity. It was recently argued that the dip feature is a strong coupling effect [2] analogous to the phonon structures observed in conventional strong-coupled superconductors. [11] Perhaps the entire spectrum beyond 2Δ requires a full microscopic d-wave model, analogous to strong-coupling theory for conventional superconductors.

V. JOSEPHSON CURRENTS

In this part of the paper, we will present and discuss Josephson currents on overdoped Bi-2212. Reproducible Josephson tunnel junctions have been obtained, indicating both quasiparticle and Josephson tunneling currents simultaneously as we displayed in Fig. 4. Josephson currents are observed at 4.2 K when the junction conductance exceeds a minimum value. For the overdoped crystals here the minimum value was about 10 μS whereas it was about 5 μS for near optimal doped Bi-2212 (Ref. 29). The hysteretic nature of the Josephson current is shown in Fig. 4(d) and the I_cR_n product for this particular junction is 3 mV. The Ambegaokar-Baratoff (A-B) theory [33] for BCS superconductors predicts the relation,

$$I_c R_n = \frac{\pi \Delta(0)}{2e} \tag{6}$$

where I_c is the Josephson current, R_n is the resistance of the junction, and $\Delta(0)$ is the energy gap at 0 K. Figure 13 shows the measured critical current I_c as function of the junction resistance R_n for 13 different SIS junctions formed on the four overdoped Bi-2212 crystals. Note that the junction resistance varies by about two decades. The solid line corresponds to the maximum theoretical value expected from A-B theory using Δ=17 meV, the average gap found in the quasiparticle data. The data show that the maximum Josephson current depends on junction resistance in a manner which is consistent with A-B theory, but with a value of $I_c R_n$ that is reduced from that expected using the average quasiparticle gap. We obtained a maximum of 7 mV for $I_c R_n$ product which is approximately 40% of the expected magnitude and the overall average is 2.4 mV. While the average $I_c R_n$ product is small compared to A-B theory it should be remembered that this theory applies to s-wave superconductors and assumes that the tunneling matrix element, $T_{\mathbf{k},\mathbf{k}'}$, is a constant, independent of electron momentum. When this type of incoherent tunneling matrix element is applied to d-wave superconductors, one obtains $I_c R_n$=0 to leading order. [34,35] This is a consequence of the changes in sign of the d-wave order parameter as one sums over momentum. Thus the $I_c R_n$ products observed here are actually quite large for d-wave superconductors. The reason for these large values is not known but it may be an indication that there is a coherent part to the tunneling matrix element, [35] that is, $\mathbf{k}$ must equal $\mathbf{k}'$ for quasiparticle states on either side of the junction. In this case the signs of the order parameters are multiplied, i.e. $(+1)^2$ or $(-1)^2$ and this leads to a non-zero Josephson current for d-wave. More experimental and theoretical work is needed to understand the magnitude of the Josephson $I_c R_n$ products observed here.

VI. SUMMARY AND CONCLUSION

We have performed PCT measurements on overdoped Bi-2212 single crystals with bulk Tc values near 62 K. High quality reproducible SIN and SIS junctions were obtained and the two junction types gave consistent results. Attempts to fit the SIS spectra to a weighted, momentum-averaged d-wave DOS led to identical gap values as found with a smeared BCS DOS but with a somewhat improved fit to the sub-gap region of the conductance. The magnitude of Δ = 15 meV-20 meV is reproducibly observed in both types of junctions on four different crystals. This gap parameter is a significant reduction from that found on optimally doped crystals ($\Delta \sim$38 meV). [1,2] The value of the strong coupling parameter, $2\Delta/k_B T_c$, is between 5.6 to 7.5, reduced from the value of 9.3 found on optimally-doped samples and this indicates a trend toward weak coupling, mean-field behavior as hole doping is increased.

The dynamic conductance spectra of the SIN and SIS junctions are qualitatively similar to those found on optimally-doped [1,2] and near optimal doped crystals [16] with all junctions exhibiting sub-gap conductance, sharp conductance peaks and a dip/hump/tail feature. The position of dip is nearly 2Δ for SIN junctions and 3Δ for SIS junctions similar to what is found for other hole doping concentrations including underdoped. [1,2] Thus the energy scale for these spectral features seems to be set by the superconducting gap value. Neither the smeared BCS DOS nor the d-wave DOS gives a good agreement with the data for eV>2Δ. In particular, we have never observed the sharp decrease in conductance for SIS junctions at eV=2Δ which is predicted by d-wave theory. It appears that the dip, hump and tail features, which are reproducibly found in these SIS spectra, are intrinsic properties of the quasiparticles in the superconducting state. These features are also found in the quasiparticle spectral weight functions measured by ARPES [30] and thus we have demonstrated an important correlation between these two measurements. What is likely needed to explain all the spectral features for eV>2Δ is a full microscopic theory, analogous to Eliashberg theory for conventional superconductors.

The sub-gap features and the conductance peaks of the SIS junctions were studied in the context of pairing symmetry. A smeared BCS DOS gives a poor fit to the data in these regions. We have also shown that a pure d-wave DOS with a constant tunneling matrix element is also not capable of fitting these particular tunnel junctions, in particular the large PHB ratio. This has forced us to assume a weighted average of the d-wave DOS with the tunnel current weighted more heavily along the (π,0) momentum direction where the d-wave gap is maximum. This improves the fit to the sub-gap region and also provides a rationale for the varying sub-gap shapes from junction to junction as being due to different weighting functions. However it is still not understood why particular tunneling directions are preferred.

Josephson currents are observed as a robust feature of the SIS junctions when the junction conductance exceeds a minimum value of about 10 μS. The maximum critical current, I_c, scales with junction resistance in a manner consistent with A-B theory for s-wave superconductors, but with a value of the $I_c R_n$ product that is reduced from that expected using A-B theory and the measured quasiparticle gap. Nevertheless, the average value of $I_c R_n$ (2.4

mV) and the maximum value (7 mV) are much larger than expected for the Josephson current between two d-wave superconductors assuming incoherent tunneling between the electrodes as is done in A-B theory. This implies that more experimental and theoretical work is necessary to understand the Josephson current between two HTS electrodes.

VII. ACKNOWLEDGMENTS

This work was partially supported by U.S. Department of Energy, Division of Basic Energy Sciences-Material Sciences under contract No. W-31-109-ENG-38, and the National Science Foundation, Office of Science and Technology Centers under contract No. DMR 91-20000.

---

[1] N. Miyakawa, P. Guptasarma, J.F. Zasadzinski, D.G. Hinks and K.E. Gray, Phys. Rev. Lett. **80**, 157 (1998); N. Miyakawa, J.F. Zasadzinski, L. Ozyuzer, et al. (unpublished).
[2] Y. DeWilde, N. Miyakawa, P. Guptasarma, M. Iavarone, L. Ozyuzer, J.F. Zasadzinski, P. Romano, D.G. Hinks, C. Kendziora, G.W. Crabtree and K.E. Gray, Phys. Rev. Lett. **80**, 153 (1998)
[3] Z.-X. Shen, D.S. Dessau, B.O. Wells, D.M. King, W.E. Spicer, A.J. Arko, D. Marshall, L.W. Lombardo, A. Kapitulnik, P. Dickinson, S. Doniach, J. DiCarlo, A.G. Loeser and C.H. Park, Phys. Rev. Lett. **70**, 1553 (1993)
[4] H. Ding, J.C. Campuzano, K. Gofron, C. Gu, R. Liu, B.W. Veal, G. Jennings, Phys. Rev. B **50**, 1333 (1994)
[5] J. R. Kirtley, C. C. Tsuei, J. Z. Sun, C. C. Chi, L. S. Yu-Jahnes, A. Gupta, M. Rupp, and M. B. Ketchen, Nature **373**, 225 (1995)
[6] C.C. Tsuei, J. R. Kirtley, Z. F. Ren, J. H. Wang, H. Raffy, and Z. Z. Li, Nature **387**, 481 (1997).
[7] C. Kendziora, R.J. Kelley and M. Onellion, Phys. Rev. Lett. **77**, 727 (1996)
[8] R.J. Kelley, C. Quitmann, M. Onellion, H. Berger, P. Almeras, G. Margaritondo, Science **271**, 1255 (1996)
[9] C. Kendziora, R.J. Kelley, E. Skelton, M. Onellion, Physica C 257, **74** (1996)
[10] T. Hasegawa, H. Ikuta and K. Kitazawa in Physical Properties of High Temperature Superconductors III ed. D.M. Ginsberg (World Scientific, 1992)
[11] E.L. Wolf, Principles of Electron Tunneling Spectroscopy (Oxford Univ. Press, New York, 1985).
[12] Q. Huang, J.F. Zasadzinski, K.E. Gray, Phys. Rev. B **42**, 7953 (1990).
[13] C. Renner and O. Fisher, Phys. Rev. B **51**, 9208 (1995).
[14] C. Renner, B. Revaz, J.-Y. Genoud, O. Fisher, J. Low Temp. Phys. **105**, 1083 (1996)
[15] R. Aoki, H. Murakami in Studies of High Tc Superconductors Vol. 20 ed. A. Narlikar (Nova Scientific, 1996)
[16] D. Mandrus, J. Hartge, C. Kendziora, L. Mihaly, L. Forro, Europhys. Lett., **22**, 199 (1993)
[17] H.J. Tao, Farun Lu, G. Zhang, E.L. Wolf, Physica C **224**, 117 (1994)
[18] Q. Huang, J.F. Zasadzinski, K.E. Gray, J.Z. Liu, H. Claus, Phys. Rev. B **40**, 9366 (1989).
[19] M. Oda, K. Hoya, R. Kubota, C. Manabe, N. Momono, T. Nakano and M. Ido, Physica C **281**, 135 (1997)
[20] M.E. Hawley, K.E. Gray, B.D. Terris, H.H. Wang, K.D. Carlson, J.M. Williams, Phys. Rev. Lett. **57**, 629 (1986).
[21] H. Won and K. Maki, Phys. Rev. B **49**, 1397 (1994)
[22] R.C. Dynes, V. Narayanamurti, J.P. Garno, Phys. Rev. Lett **41**, 1509 (1978).
[23] A.F. Andreev, Zh. Eksp. Theor. Fiz. **46**, 1823 (1964)
[24] S. Kashiwaya, Y. Tanaka, M. Koyanagi, K. Kajimura, Phys. Rev. B **53**, 2667 (1996)
[25] G.E. Blonder, M. Tinkham and T.M. Klapwijk, Phys. Rev. B **25**, 4515 (1982)
[26] N. Tsuda, K. Nasu, A. Yanase, K. Siratori, Electronic Conduction in Oxides (Springer, 1991).
[27] Z. Yusof, J.F. Zasadzinski, L. Coffey and N. Miyakawa, Phys. Rev. B **58**, 514 (1998)
[28] P.J. White, Z.-X. Shen, C. Khim, J. M. Harris, A. G. Loeser, P. Fournier, A. Kapitulnik, Phys. Rev. B **54**, R15669 (1996)
[29] P. Romano, J. Chen and J.F. Zasadzinski, Physica C **295**, 15 (1998)
[30] M.R. Norman, H. Ding, J. C. Campuzano, T. Takeuchi, M. Randeria, T. Yokoya, T. Takahashi, T. Mochiku, K. Kadowaki Phys. Rev. Lett. 79, 3506 (1997); Z.X. Shen, P. J. White, D. L. Feng, C. Kim, G. D. Gu, H. Ikeda, R. Yoshizaki, and N. Koshizuka, Science 280, **259** (1998)
[31] P. Mallet, D. Roditchev, W. Sacks, D. Defourneau, J. Klein Phys. Rev. B **54**, 13324 (1996)
[32] C. Manabe, M. Oda, M. Ido, J. of the Phys. Soc. of Japan **66**, 1776 (1997)
[33] V. Ambegaokar and A. Baratoff, Phys. Rev. Lett. **10**, 486 (1963)
[34] Yung-mau Nie, L. Coffey Phys. Rev. B **57**, 3116 (1998)
[35] R. A. Klemm, G. Arnold, C. T. Rieck and K. Scharnberg (unpublished)

FIGURE CAPTIONS

Figure 1. Schematic representation of SIS junction formed by a Au tip.

Figure 2. Dynamic conductance of three SIN junctions [dots], from three different overdoped Bi-2212 (T_c=62 K) crystals at 4.2 K. Negative bias region corresponds to occupied states in the DOS. The solid lines are estimated normal state conductances (σ_n^*) which are generated from verifying the sum rule of the DOS.

Figure 3. Normalized conductance of three SIN junctions [dots], which are given in Fig. 2. The solid lines are BCS DOS fit which include smearing factor Γ. Δ and Γ values are given in the figure for each fit.

Figure 4. The current-voltage characteristics of three different SIS junctions. (d) is expanded scale of (c) near zero bias for clarity. (d) shows hysteretic zero-bias feature which indicates a Josephson current.

Figure 5. The tunneling conductance of SIS junctions for overdoped Bi-2212. The upturn around ±300-400 mV may indicate that the bias is approaching the barrier height. The sub-gap tunneling conductance can not be seen, because of switching.

Figure 6. The normalized tunneling conductance of SIS junctions [dots]. (a) and (b) are the same data with Fig. 5 (a) and (b). Figure 6 (c) is a different junction. The normalizations are conducted by a constant value which are chosen at 150 mV. The solid lines are BCS fits, which are calculated using given Δ and Γ values at graph and T=4.2 K.

Figure 7. The positive bias part of the tunneling conductance of SIS junction [dots]. Relatively small Josephson current helped to reveal sub-gap conductance very clearly. The solid line is an estimated normal state conductance. The inset shows full spectrum.

Figure 8. The normalized conductance [dots] of the junction which is shown in Fig. 7. The solid line is an SIS fit for BCS superconductor, which is calculated for Δ=17.5 meV, Γ=1.4 meV and T=4.2 K.

Figure 9. The momentum-averaged DOS for a superconductor with $d_{x^2-y^2}$ pairing symmetry (a). The convolution of (a) with itself produces an SIS tunneling conductance (b).

Figure 10. The normalized conductance [dots] of the junction which is shown in Fig. 7. The solid line is an SIS fit for a d-wave superconductor with weighting, $f(\phi) = 1 + 0.8cos(4\phi)$, which is calculated for Δ=17.5 meV, Γ=0.05 meV and T=4.2 K.

Figure 11. The positive bias part of the tunneling conductance of another SIS junction [dots]. The solid line is an estimated normal state conductance. The inset shows full spectrum.

Figure 12. The normalized conductance [dots] of the junction which is shown in Fig. 11. The solid line is an SIS fit for a d-wave superconductor with weighting, $f(\phi) = 1 + 0.6cos(4\phi)$, which is calculated for Δ=19.5 meV, Γ=1.5 meV and T=4.2 K.

Figure 13. Josephson current versus junction resistance for overdoped Bi-2212 at 4.2 K [dots] in logaritmic scale. The solid line is Ambegaokar-Baratoff prediction for Δ=17 meV.

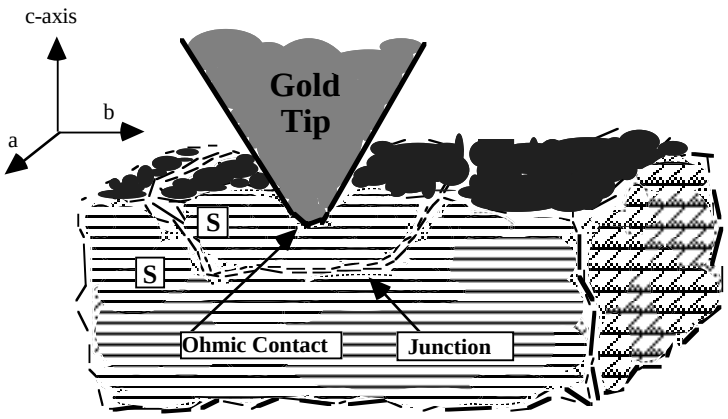

Fig. 1 L. Ozyuzer et al.

Fig. 2 Ozyuzer et al.

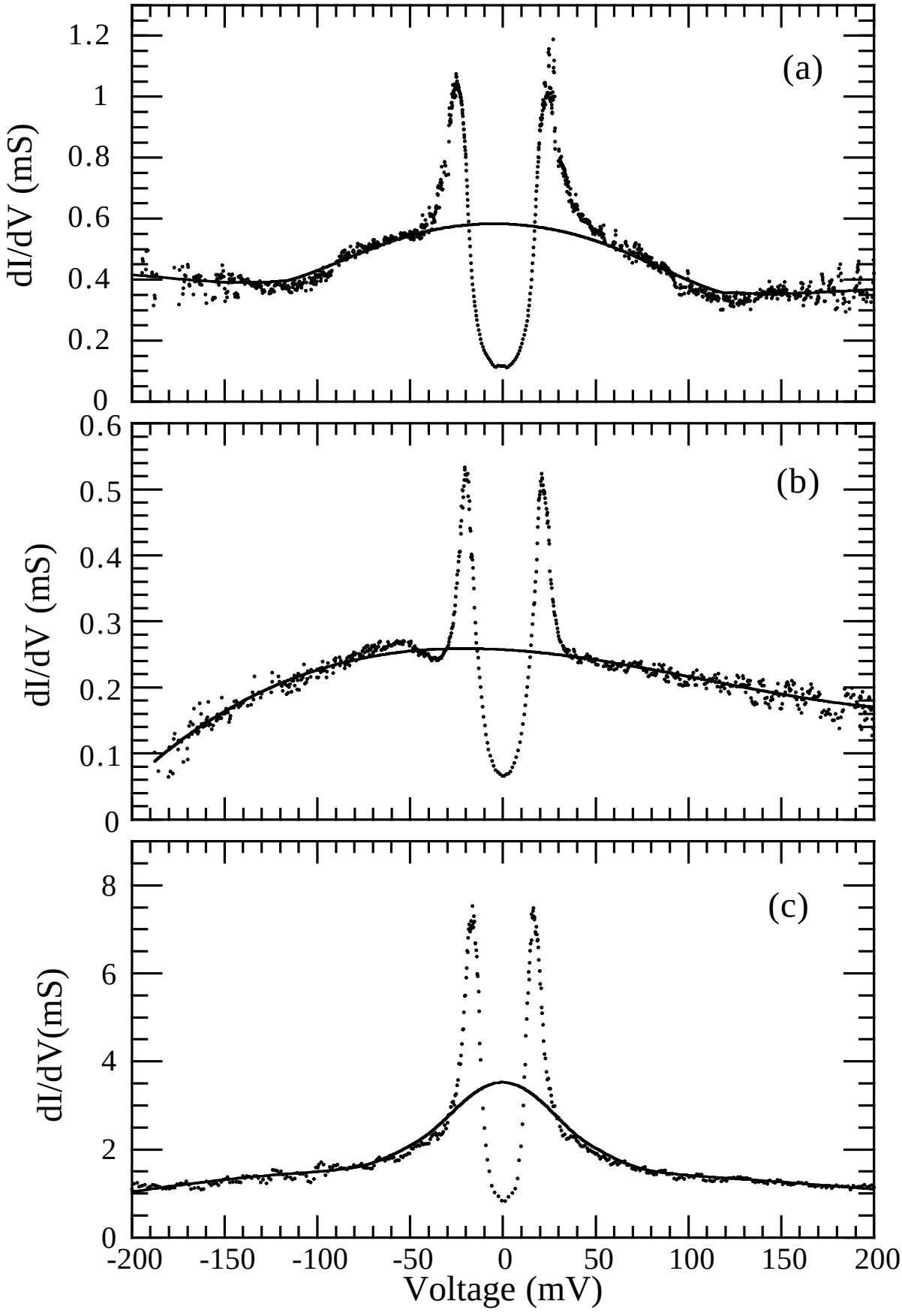

Fig. 3 Ozyuzer et al.

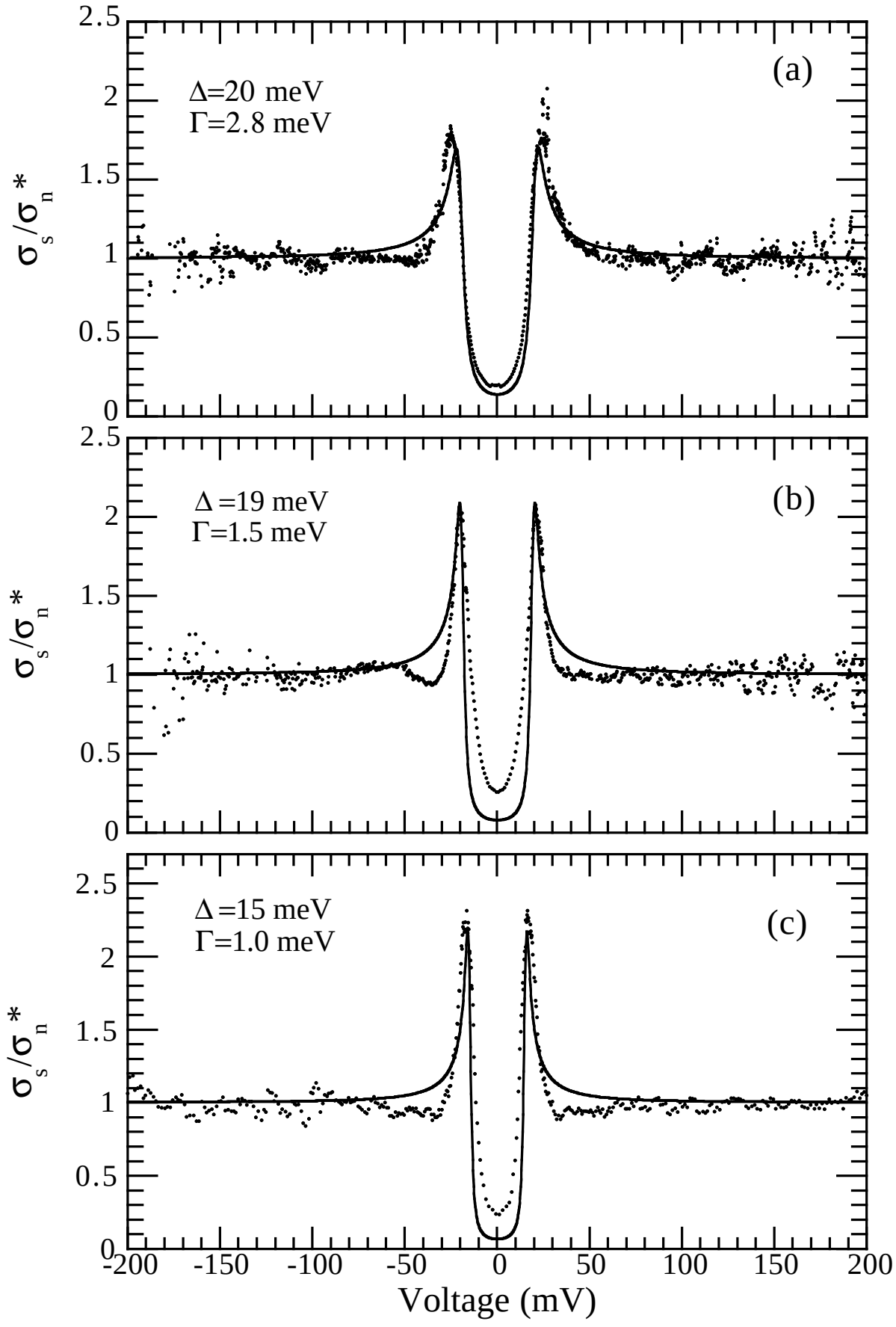

Fig.4 Ozyuzer et al.

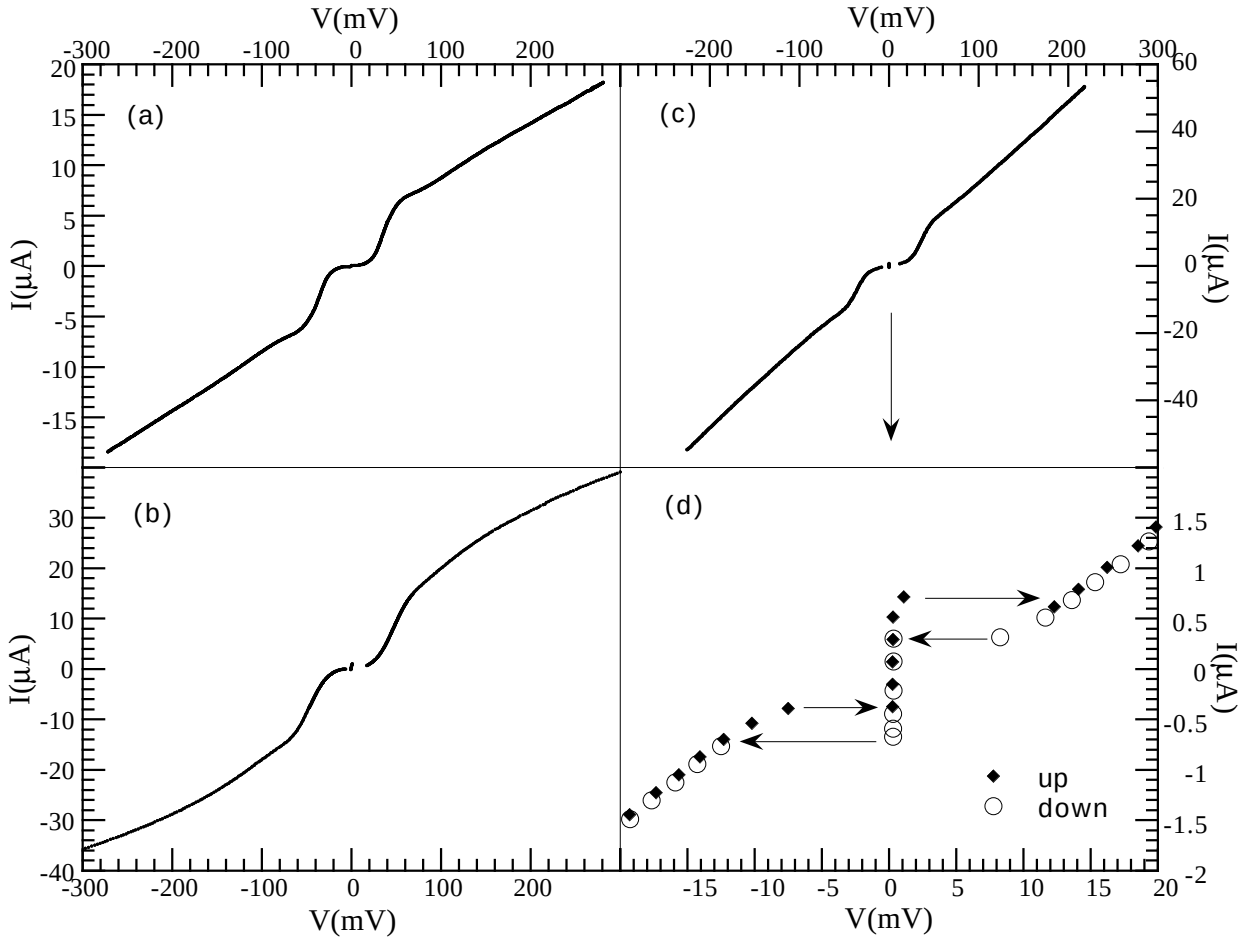

Fig. 5 Ozyuzer et al.

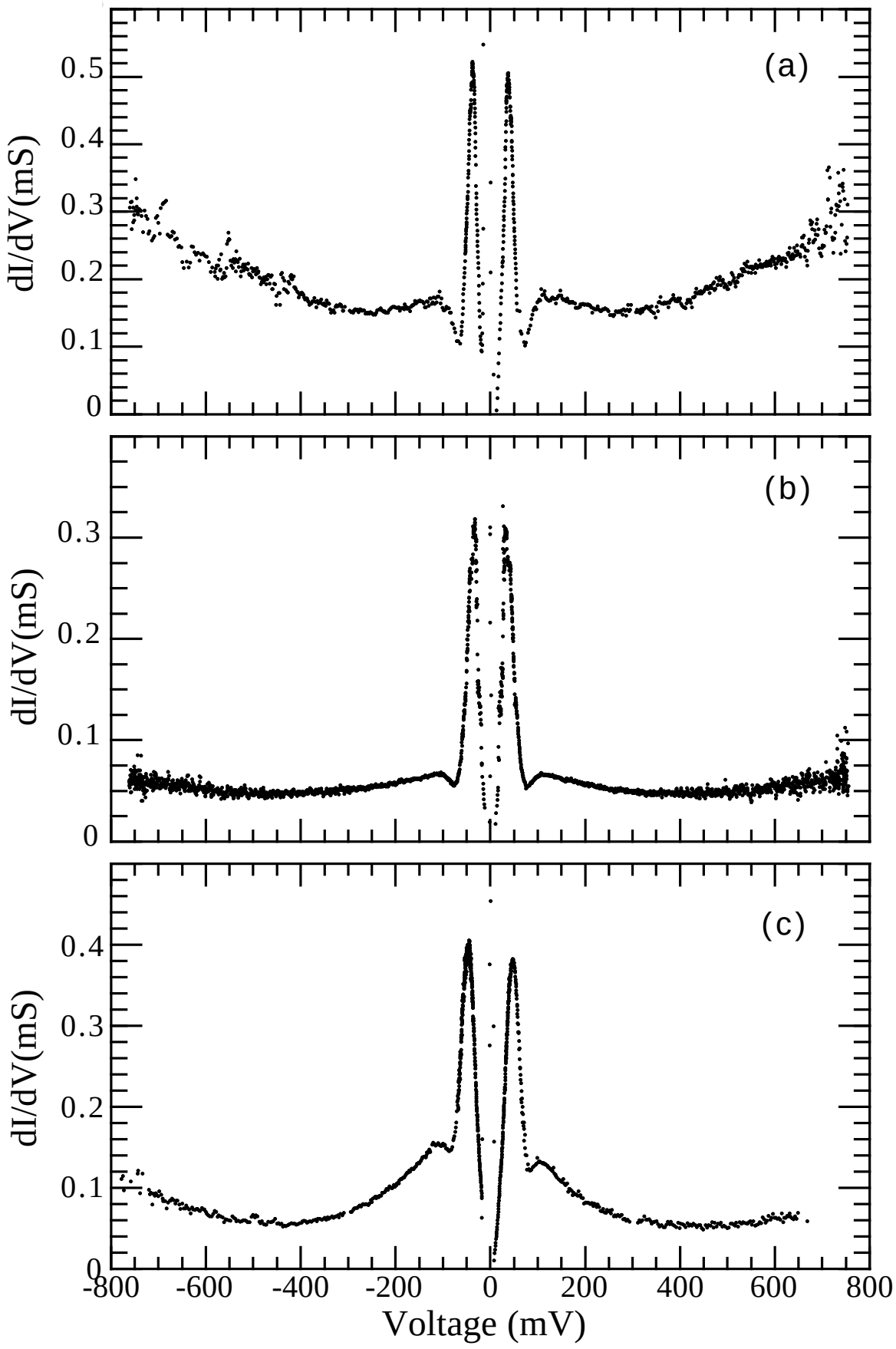

Fig. 6. Ozyuzer et al.

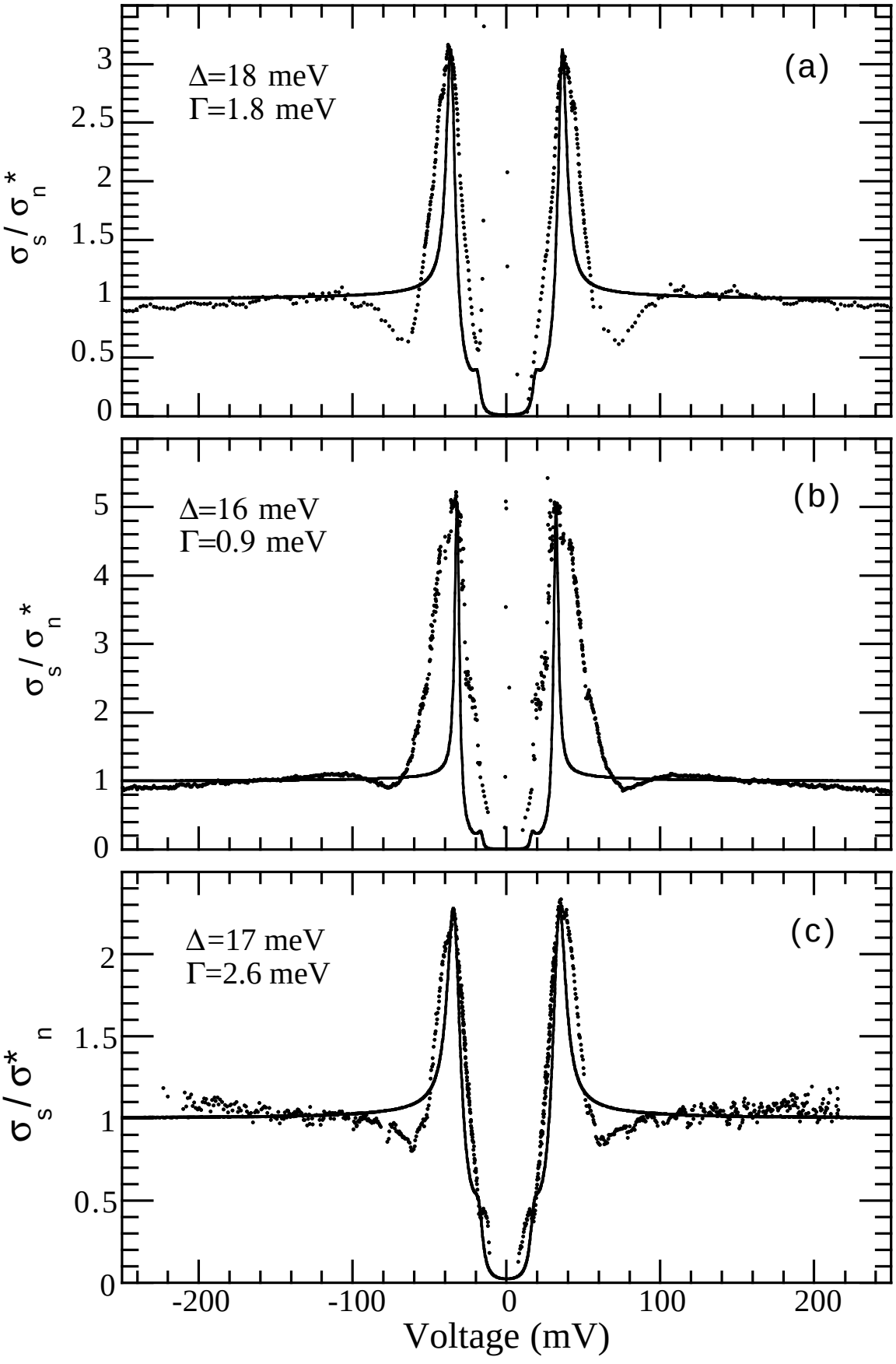

Fig. 7 Ozyuzer et al.

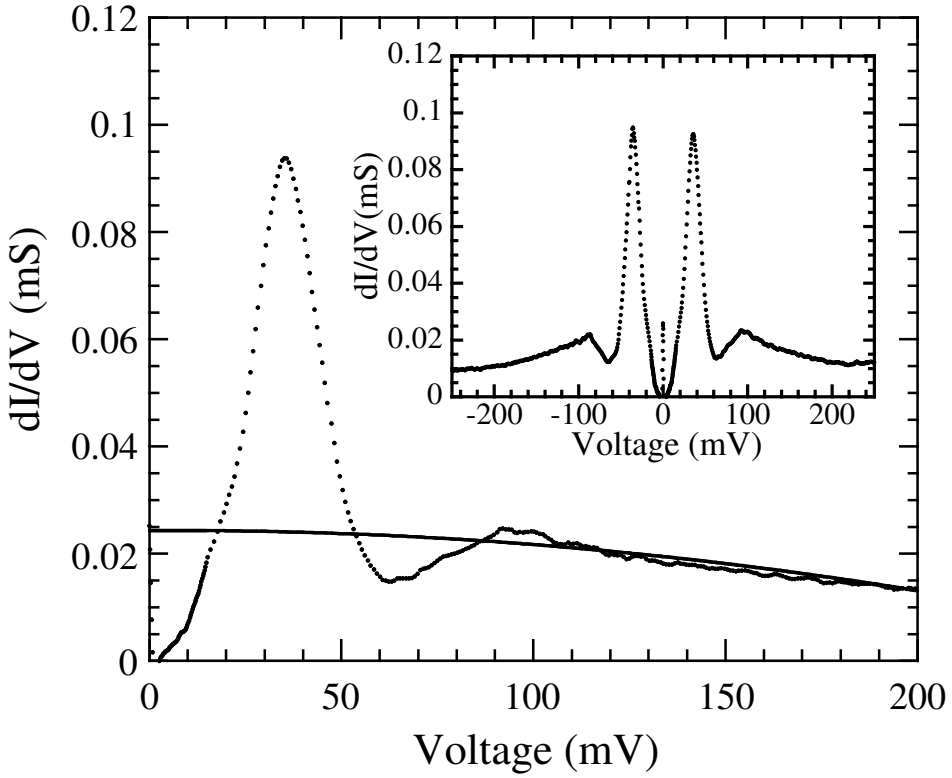

Fig. 8 Ozyuzer et al.

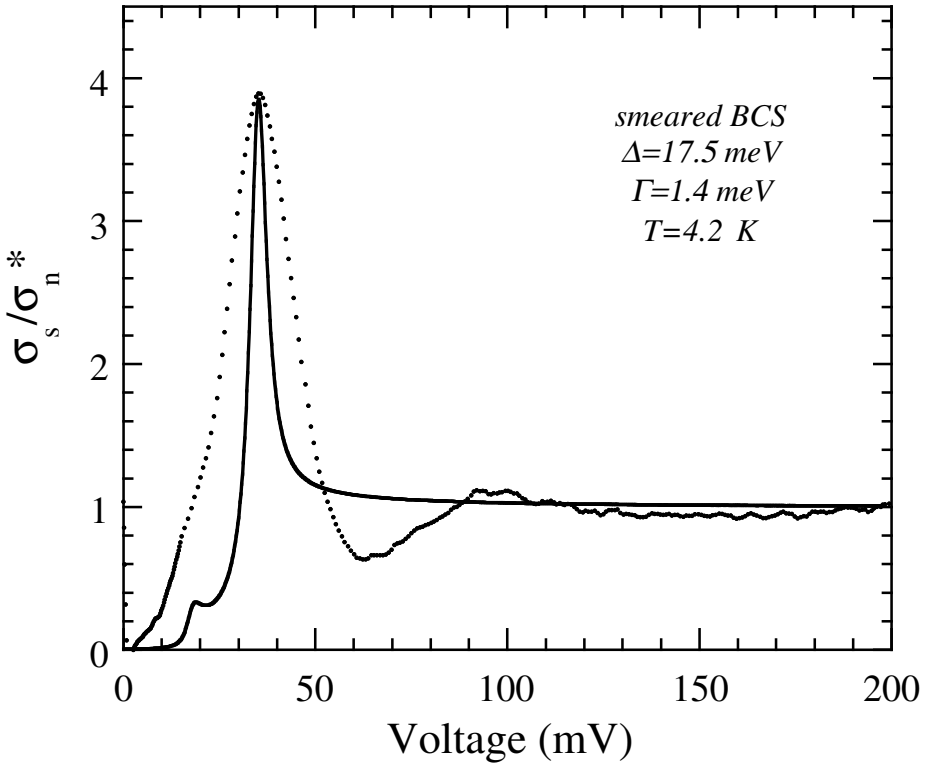

Fig. 9 Ozyuzer et al.

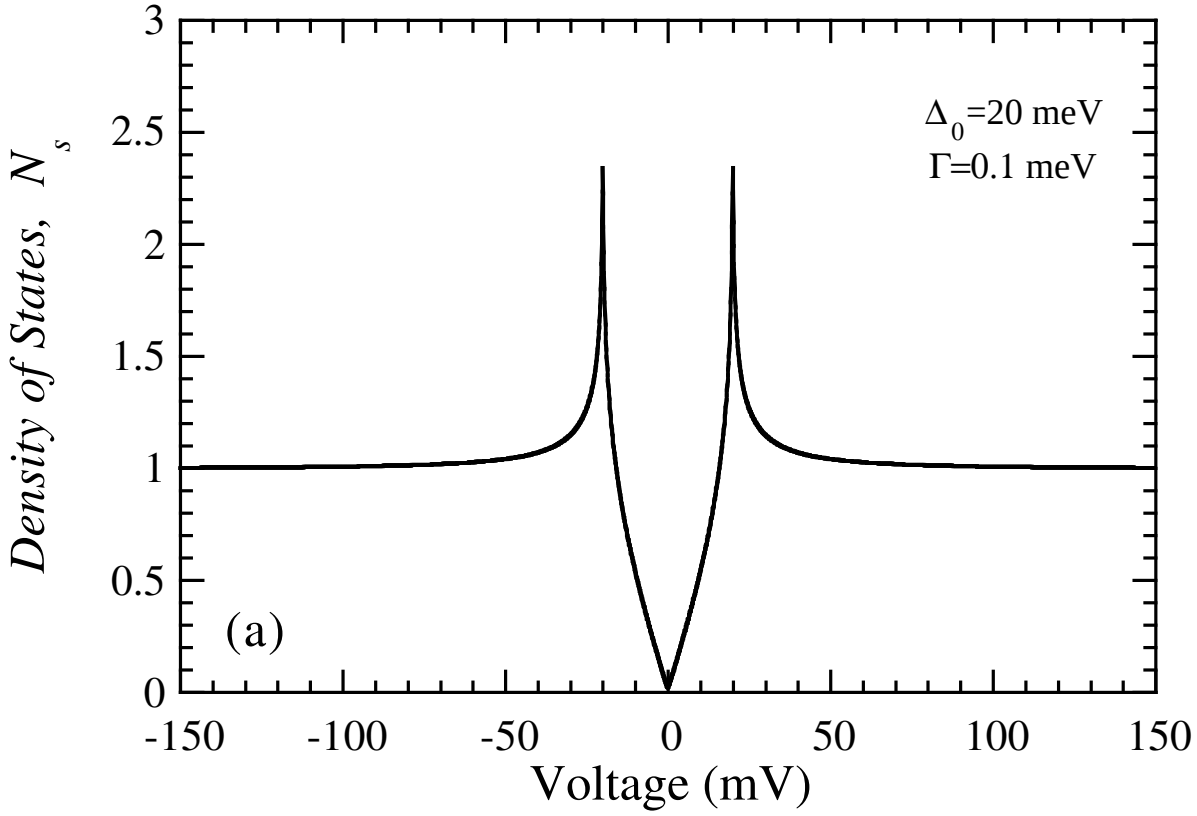

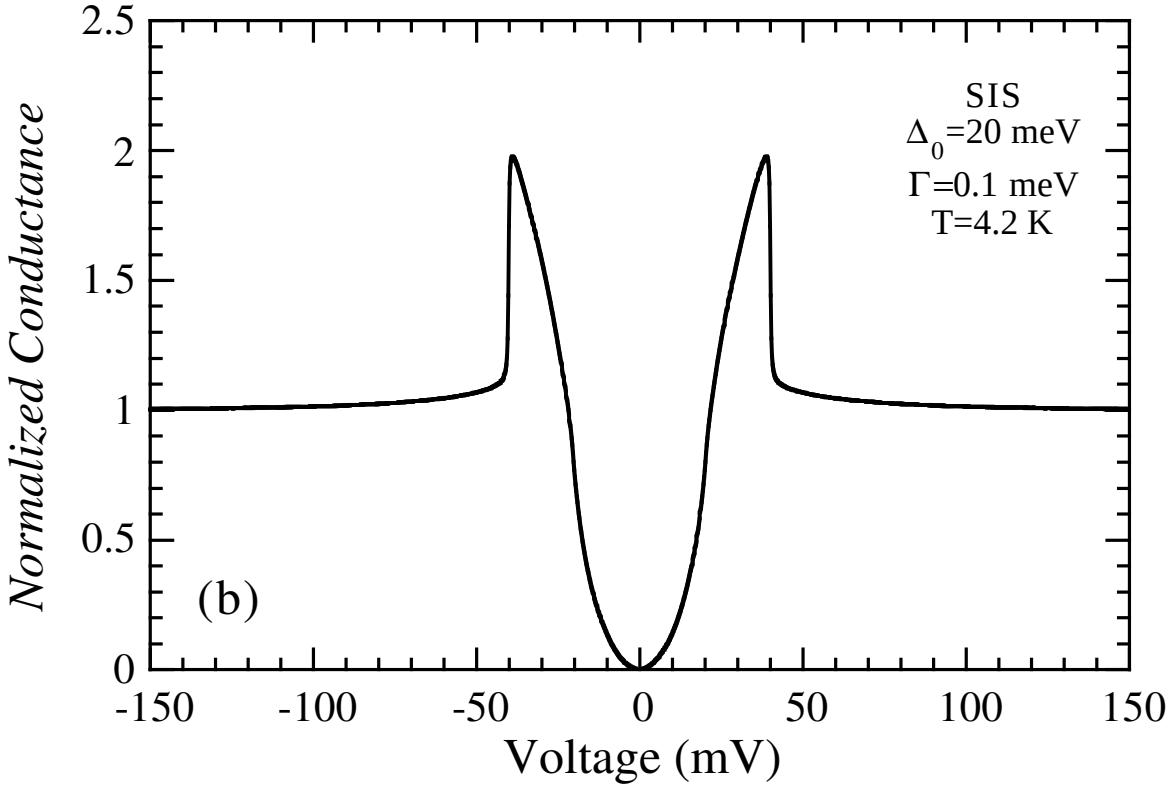

Fig. 10 Ozyuzer et al.

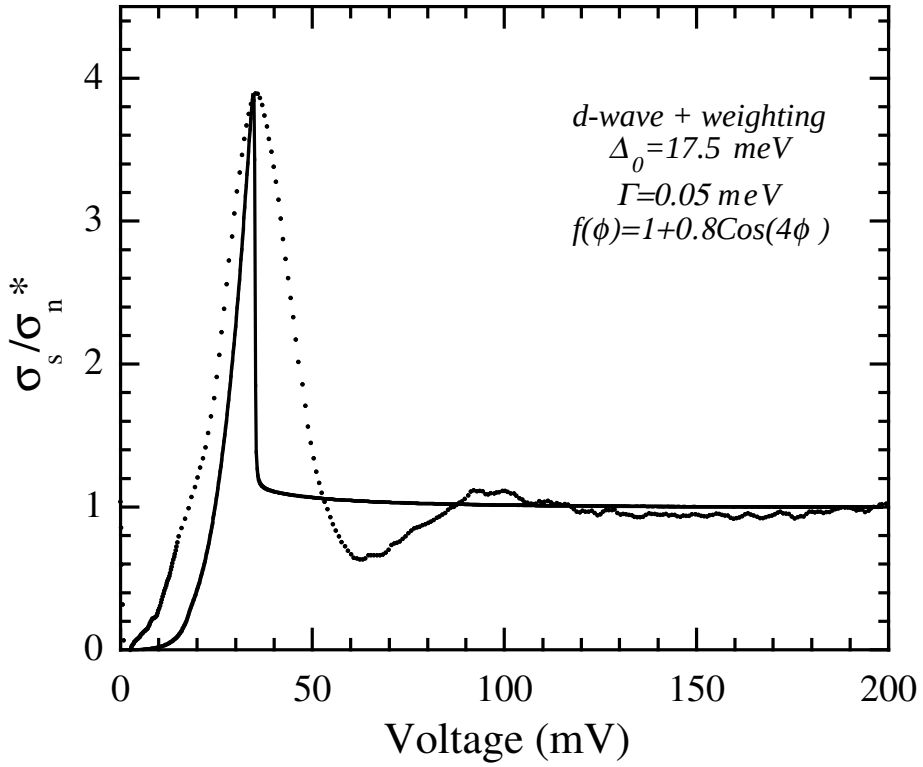

Fig. 11 Ozyuzer et al.

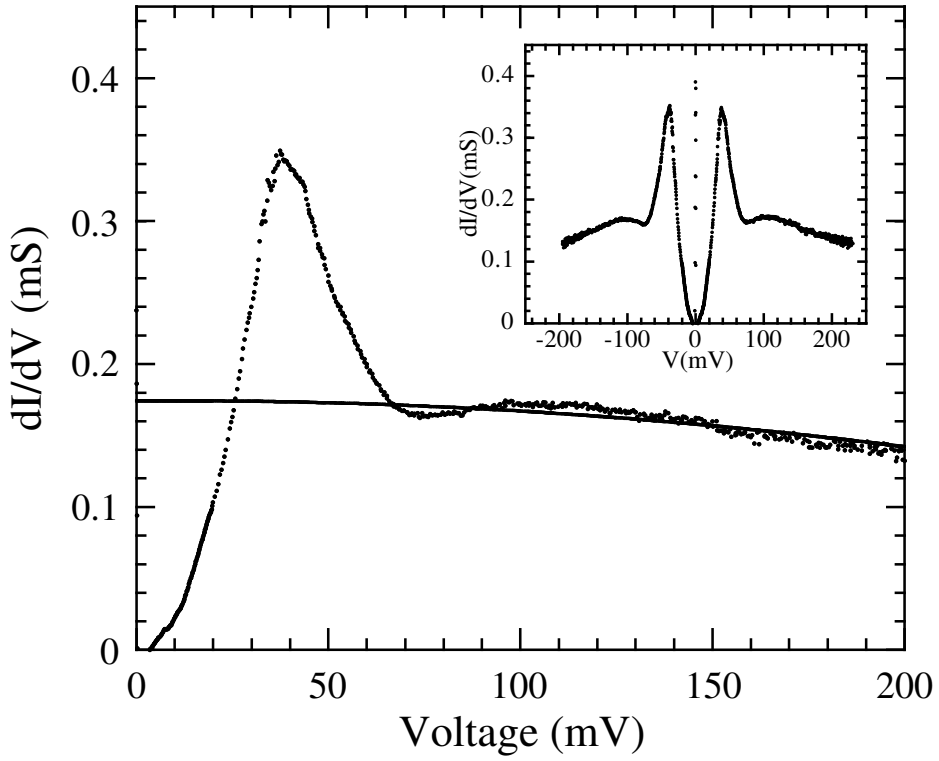

Fig. 12 Ozyuzer et al.

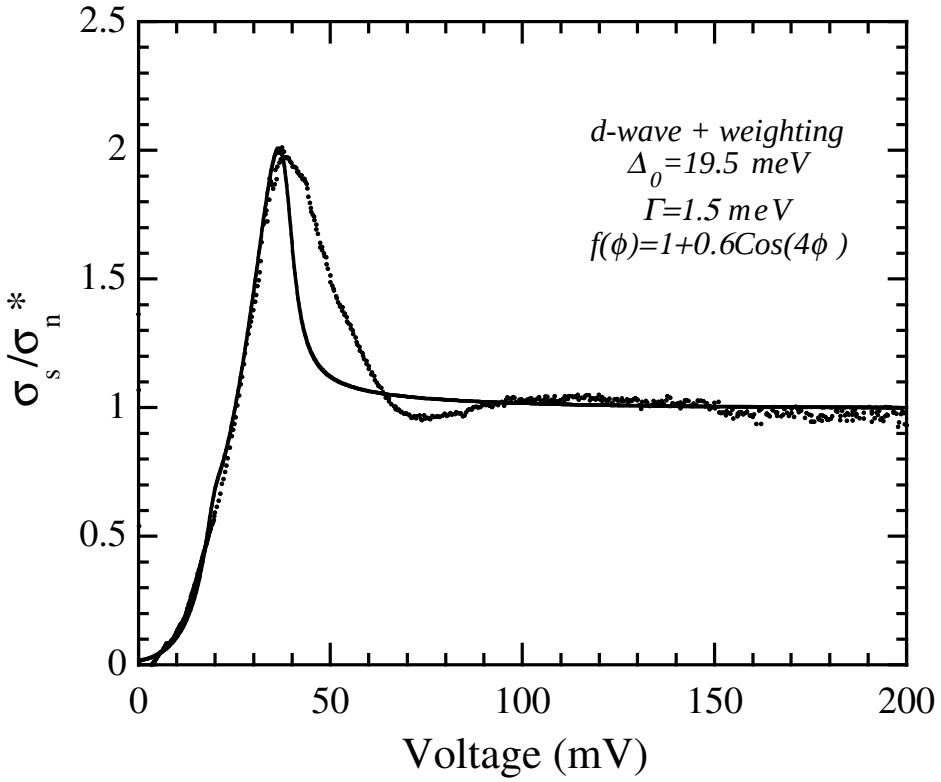

Fig. 13 Ozyuzer et al.